JOURNAL OF MATERIALS SCIENCE 31 (1996) 6515–6522

Mechanical properties of optically transparent, multi-layered laminates

SEUNGGU KANG
Departments of Materials Science and Engineering, Kyonggi University, Suwon, Kyonggi-Do, 442-760, Korea
KOOKYUN BYUN, DELBERT DAY*
*Department of Mechanical Engineering and *Graduate Center for Materials Research, University of Missouri-Rolla, Rolla, MO 65401, USA*

The objective of this investigation was to study how the mechanical properties of an optically transparent composite varied with the geometrical arrangement, stacking sequence, of polymethylmethacrylate (PMMA) (designated as P) and composite (designated as C) layers. The multi-layered composites (about 6.63 mm thick) were highly transparent between 22 to 46 °C in the visible region. As expected, the sandwich structure, (CCPP)s had the highest Young's modulus while (PCCP)s and (PPCC)s composites had the highest flexural strength and work of fracture, respectively. The flexural strength of these laminated composites, which contained only 0.8 vol % fibre without any coupling agent, was up to 21% higher than that of pure PMMA.

The stress distribution through the thickness at the midpoint of a sample loaded in three-point bending was computed by the finite element method (FEM). The computed stress distribution allowed the expected point of failure to be established. The relationship between the stacking sequence, stress level under a given load, and strength was also investigated. The observed fracture modes were complex and the maximum stress failure criterion did not fit these composites. The fracture was always complex (tensile and shear), starting with tensile failure followed by shear mode (delamination) and another tensile mode. The first crack always commenced at a PMMA layer adjoining the composite layer which contained the highest stress. The optimum stacking sequence when such composites are used as a window is concluded to be (PCCP)s, since this sequence had the highest flexural strength (141 MPa) and a moderate work of fracture (37 kJ m^{-2}).

1. Introduction

Highly transparent polymethylmethacrylate (PMMA) composites reinforced with up to 10 vol % of glass fibre have been made by a lamination process [1, 2]. The optical transparency of these composites was achieved by matching the refractive indices of the fibre and PMMA matrix and developing a prepreg which allowed the polymer matrix to thoroughly wet and coat the fibres. However, to apply this composite material to real systems (i.e. aircraft canopies, automobile windshields), laminating the thin prepregs (< 0.05 mm) to appropriate thickness (6 to 12 mm) might be harmful to the optical properties of the composite due to the large number of potential interfaces which could cause light scattering and optical distortion.

Recently, sandwich type composites composed of composite prepregs laminated to each side of a PMMA core have been utilized [3] so that reasonable thicknesses and higher flexural strengths could be obtained without harming the optical transmission. Originally, the purpose behind the sandwich composites was to separate two strong and stiff, but relatively thin composite plates by a thick, but light weight "core" [4, 5]. This structure has a higher moment of inertia for a given weight and is, therefore, used in applications where a high stiffness-to-weight ratio is required. It should be noted that, in an optical system, there are additional requirements, e.g. a high transparency-to-thickness ratio, strength-to-weight ratio and work of fracture per unit area.

In the present study, the dependence of the flexural strength of multi-layer laminated composites on the stacking sequence of glass fibre prepregs and PMMA plates was investigated. A pure PMMA beam and six multi-layered composite beams composed of different stacking sequences were fabricated and measured. First, the optical transparency of the composite was investigated as a function of temperature and wavelength. The flexural strength, work of fracture and Young's modulus of these specimens was evaluated from three-point bending tests. The normal stress distribution through the thickness at the mid-point of the specimens was calculated by the finite element

0022–2461

method (FEM). Finally, the fracture surfaces of broken specimens were examined by optical microscopy and scanning electron microscopy (SEM) to relate the stress distribution through the thickness of the specimen to the flexural strength.

2. Experimental procedure

2.1. Glass fibre and prepreg preparation

BK10 bulk glass was re-melted and fined for 45 min at 1250 °C in a resistance heated Pt/Rh 10-hole bushing. BK10 fibres, with an average diameter of 15 μm, were drawn at 1204 °C and 4.0 m s^{-1}. The refractive index (n_D) of the fibres was 1.4904 ± 0.0003 and that of the PMMA was 1.4924 [2]. Strips of fibres were prepared by moving a rotating collection drum at a controlled speed in a horizontal direction normal to the fibre pulling direction. PMMA dissolved in MMA (1:9 in wt %) was sprayed on the fibres as they pulled, but no coupling agent was applied to the fibres.

The fibre volume per cent could be varied by either changing the translation speed of the collection drum or the amount of PMMA sprayed on the fibres. The carefully prepared PMMA/BK10 glass fibre prepreg layers were approximately 0.033 mm thick and contained about 9.8 vol % of BK10 glass fibres (measured by a burn-off test). Uneven surfaces which lower the transparency of the prepreg, due to reflection and light scattering, were eliminated by hot-pressing the prepregs between smooth glass plates.

2.2. Manufacturing multi-layered composites

Each multi-layer laminated composite consisted of four PMMA plates (each was 1.53 ± 0.05 mm thick and hereafter denoted as "P") and four composite layers (one composite layer is hereafter denoted as "C"). Each composite layer consisted of four prepreg layers. The unidirectionally reinforced multi-layered composite specimens (total thickness of 6.63 ± 0.22 mm) were prepared by hot-pressing P and C layers between glass plates (152.4 mm × 101.6 mm) at 140 °C for 5 h at 0.7 MPa. For three-point bending tests, specimens were cut (length = 10 cm, span = 8 cm and breath = 1 cm) from a multi-layered composite plate. The cut surfaces were polished using sandpapers up to # 600 grit. The stacking sequences are expressed in the following way; the PCPCCPCP sequence is expressed as (PCPC)s, where "s" implies symmetric to the neutral axis. While each prepreg layer contains 9.8 vol % of glass fibres, the multi-layered composites consisting of four PMMA plates and four composite layers contain only 0.8 vol % of glass fibres (as measured by the burn-off test).

2.3. Optical transmission

Transmission was measured as a function of temperature and wavelength in the visible region (350 nm to 750 nm) using a spectrophotometer Beckman Model 26. The transmission was measured by placing a sample of the laminated composite in a cell filled with Laser Liquid (n_D = 1.4940 ± 0.0002) to reduce the effect of surface roughness.

2.4. Flexural strength

The flexural strength and modulus were measured according to ASTM test method D790-81 using an Instron Model 4204 Load Machine. Each multi-layered composite beam specimen, rectangular cross-section, was loaded in three-point bending in a direction perpendicular to the unidirectionally oriented fibres. The span to depth ratio (L/d) was 12, span to width ratio (L/b) was 8 and loading head speed was 5 mm min^{-1}.

The flexural strength was calculated from Equation 1

$$\sigma_f = 3PL/2bd^2 \quad (1)$$

where, σ_f = flexural strength, P = failure load, L = span, b = width of sample, and d = depth of sample.

The modulus of elasticity is the ratio of elastic stress to the corresponding strain. It was calculated by drawing a tangent to the steepest initial straight-line portion of the load-deflection curve, and using Equation 2

$$E_{(b)} = P'L^3/4\delta bd^3 \quad (2)$$

where, $E_{(b)}$ = modulus of elasticity in bending, P' = applied load in the linear portion of the load-deflection curve, and δ = deflection corresponding to the load, P'.

2.5. Work of fracture

The work of fracture is the amount of work required to break the bar in three-point bending and has been defined [6] as the amount of energy used to create new fracture surfaces in exchange for stored elastic energy. It was calculated by dividing the area under the load-displacement curve by the cross-sectional area of the bar at the point of fracture to give a normalized value with the units kJ m^{-2}.

2.6. Stress distribution analysis

The stress distribution in the specimen during flexural loading was calculated for each composite and for an unreinforced PMMA plate by a 3-D finite element method (FEM) using the commercial package NASTRAN. The number of elements generated by a self-authored program for the finite element method was 40 × 2 × 8 = 640, the shape of each element was orthorhombic and the number of nodes was 41 × 3 × 9 = 1107. Input engineering properties for this analysis are listed in Table I. Poisson's ratio for the BK10 glass fibre (estimated value was 0.24) was obtained by the regression method on the assumption that it is inversely proportional to the SiO_2 content of the silicate glass. For most silica glass fibres, ν is in the range of 0.23 to 0.27 [7] (85 wt % SiO_2 in BK10).

PMMA/BK10 glass fibre prepregs can be considered transversely isotropic, since fibres are unidirectionally oriented. Therefore, the engineering

TABLE I Engineering properties for PMMA BK10 glass fibre (15.0 ± 2.3 μm diameter)

	PMMA	BK-10 fibre
Young's modulus (GPa)	3.1	53
Poisson's ratio	0.35	0.24
Shear modulus (GPa)	1.2	21.4[a]

[a] Calculated from $G_f = E_f/2(1 + \nu_f)$.

properties were calculated from the following equations

$$E_1 = V_f E_f + V_m E_m \quad (3)$$

$$E_2 (= E_3) = E_f E_m/(V_f E_m + V_m E_f) \quad (4)$$

$$G_{12} = G_f G_m/(V_f G_m + V_m G_f) \quad (5)$$

$$\nu_{12} = V_f \nu_f + V_m \nu_m \quad (6)$$

where E_1 = Young's modulus in a fibre direction, V_f = vol % glass fibre, E_f = Young's modulus of glass fibre, V_m = vol % matrix, E_m = Young's modulus of matrix, E_2 = Young's modulus in a transverse of fibre direction (parallel to sample breadth), E_3 = Young's modulus parallel to sample thickness, G_{12} = in-plane shear modulus, G_f = shear modulus of glass fibre, G_m = shear modulus of matrix, ν_{12} = major Poisson's ratio, ν_f = Poisson's ratio of glass fibre and ν_m = Poisson's ratio of matrix.

2.7. Fracture surface

Surfaces fractured in the flexural test were examined by optical microscopy and scanning electron microscopy (SEM) using a Jeol Model 35CF, to locate the fracture initiation point and evaluate the fracture propagation behaviour.

3. Results and discussion

3.1. Optical properties

Highly transparent, multi-layered composites were produced by the carefully tailored processing procedure used in the present work. A comparison of the transmission for a pure PMMA plate and multi-layered composites is shown in Fig. 1(a). The transmission (at 589.3 nm) for the 6.44 mm thick pure PMMA specimen was 93% and was 85.0 ± 3.6% between 9 and 46 °C for the 6.63 ± 0.22 mm thick multi-layered composites (Fig. 2). The optical transmission should not depend upon the P–C stacking sequence, thus, the small difference in transmission for the different laminated composites may come from processing differences such as imperfect fibre wetting or variable prepreg thickness. Nevertheless, all of these samples have a high transmission compared to normal glass fibre composites.

3.2. Stress distribution and flexural properties

In multi-layer laminated composites, each layer in a composite has a different strength. Thus, the

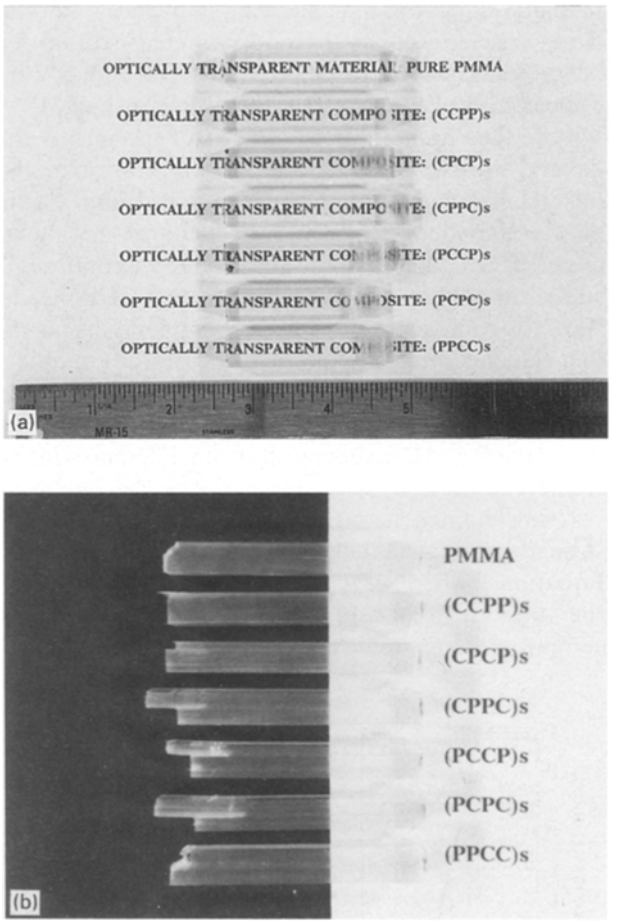

Figure 1 The optically transparent multi-layered composites: (a) flat-wise display for broken multi-layered composite (6.63 ± 0.22 mm thick) and PMMA beam (6.44 mm thick) specimens; (b) edge-wise display. Notice that this side was polished with # 600 grit, resulting in a translucent surface.

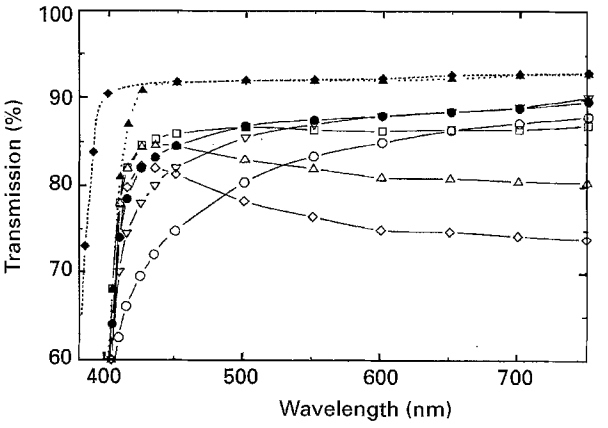

Figure 2 Percent transmission of (PCCP)s specimen as a function of wavelength at the temperature shown. This sample is 6.64 mm thick and contains four composite layers (i.e. 16 layers of prepreg of 9.8 vol % glass fibre). ○ 9.3 °C; ▽ 25.6 °C; ●33.6 °C; □ 45.9 °C; △ 57.3 °C; ◇ 62.4 °C. PMMA; ◆ Rohm & Haas; ▲ 3 M.

flexural-load-carrying capacity of laminated composites depends upon the stress level in each layer during the bending test. In other words, crack initiation occurs in that layer where the stresses exceed that layer's flexural strength. Therefore, knowledge of the stress distribution through the thickness of the specimen under flexural loading is very important for

predicting the optimal stacking sequence. Normal stress distributions at the midspan cross-section for beam specimens at a flexural load of 25 kg, were calculated by FEM (see the dotted line in Fig. 3).

For the homogeneous PMMA specimen, the flexural stress varies linearly from compression on the top to tension on the bottom as expected from elastic pure beam theory. Multi-layered composites, however, show a highly non-linear and discontinuous stress distribution, especially for (PCCP)s and (PCPC)s composites, see Fig. 3(d) and (e). This means that the maximum stress may not occur at the outermost surface layer of the specimen. Note that the discontinuous stress distribution at the interface between the P and C layers results from differences in the stiffness of these layers.

Using homogeneous beam theory, the flexural strength was calculated for three-point loading from Equation 1 where σ_f is the calculated maximum tensile stress at failure. In the case of a unidirectional composite laminate, it can be assumed to be homogeneous along the z-axis (perpendicular to the fibre direction). However, the maximum stress does not always occur at the outermost layer in a multi-layer polymer–composite laminate as shown in Fig. 3. Thus, Equation 1 gives only an apparent strength value (compare the outer stress by FEM in Table IV with flexural strength from Equation 1 in Table II).

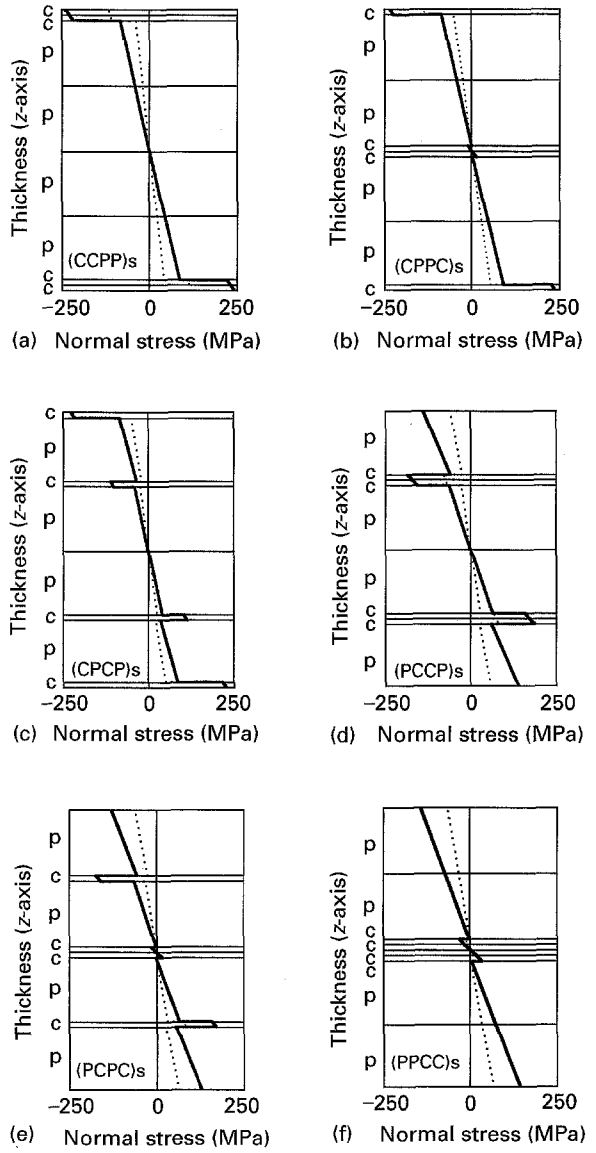

Figure 3 Stress distribution through the multi-layered composite thickness for six different P–C stacking sequences. The dotted line and solid line denote the stress distribution at 25 kg load and at the failure load, respectively.

In Table II, the multi-layered composite specimens are arranged in the order of increasing deflection calculated at a given load of 25 kg. The values in Table II are the average of three individual specimens for each type of composite. The results fall into two groups, samples where the composite layer is the outer layer of the specimen (denoted as C-out group) and where the polymer layer is on the outside (denoted as a P-out group). The C-out group had a slightly smaller deflection at a given load. Within each group, there is a decrease in flexural strength as the deflection increases (from (CCPP)s to (PPCC)s) for a 25 kg load. Table III shows the stresses from bottom to neutral axis at several nodes for a flexural load of 25 kg.

As expected from the sandwich structure concept, the (CCPP)s specimens in Table II had the highest Young's modulus, while (PPCC)s specimens, which are the reverse structure, had the lowest Young's modulus. The C-out group is superior to the P-out group from the standpoint of a high Young's modulus. The (CCPP)s samples have a Young's modulus which is 1.5 and 1.8 times greater than that for the (PCCP)s and (PPCC)s composites, respectively. However, it is evident that the C-out group, except (CCPP)s, has a smaller flexural strength than the P-out group. The flexural strength for the (CCPP)s composites is up to 14% higher than that of the unreinforced PMMA, but the increase is 21% for the (PCCP)s composites. When the low fibre vol% (0.8%) for these multi-layered composites is considered, the increase in flexural strength is impressive. Less than 1% fibre increases the flexural strength by 21%. In a structural design where a high stiffness-to-weight ratio is required, the (CCPP)s sandwich construction offers the best combination of properties for the sequences studied. In a special application like an aircraft canopy, stiffness will not be the only requirement. An aircraft canopy requires high strength and high stiffness as well as high work-of-fracture. The work-of-fracture for the P-out group was much greater than that of the C-out group. The (PPCC)s specimens had the highest work-of-fracture, four times that of the (CCPP)s sandwich structure. From this point of view, one of the P-group structures could be selected for special purposes so that it gives a high strength and high work-of-fracture with reasonably good stiffness.

Within each group, differences in strength, which are fairly small, could be explained according to the probability of fracture related to the stress level occurring during flexure. Table III shows the flexural stresses at selected locations for a load of 25 kg. In determining the failure strength of a specimen, the layer to fail first dominates. For a given load, a specimen containing a higher stress at the layer failing first is expected to have a higher probability of fracture. By examining the fracture surfaces (Section 3.3), the first

layer to fracture can be determined and is marked with a 'b' in Tables III and IV. In Fig. 4, the calculated flexural strength from Equation 1 is plotted as a function of the stress in that layer where fracture is believed to have first occurred. There is a linear relationship for each group of specimens (P-out and C-out), but they seem to have different slopes. The negative slopes indicate that the specimen which experienced higher stress during the flexural loading has lower strength due to higher probability of breaking. The steeper slope for the C-out group indicates that the strength of C-out specimens is more sensitive to the stress level, therefore, the C-out specimens, except the (CCPP)s specimen, have weaker strength than that of the P-out group specimens.

3.3. Fractography

Fracture surfaces were examined microscopically and visually. Generally in three-point bending, the type of failure modes observed can be classified as: tensile, shear or complex failure [8]. For tensile failures, the fracture surface is nearly flat, a shear failure causes debonding of the fibre from the matrix, and a complex failure shows both fibre debonding and constituent (fibre and matrix) failures. More practically, the failure mode can depend on the span to depth ratio (L/d) [8]. Rearranging Equation 1 as

$$\sigma_{max} = 3PL/2bd^2 = 3P/2bd(L/d) \quad (8)$$

$$\tau_{max} = 3P/4bd \quad (9)$$

where, τ_{max} is maximum shear stress.

From Equations 8 and 9, σ_{max} in the beam decreases with decreasing L/d ratio and τ_{max} (at the neutral axis) is not affected by the L/d ratio. τ_{max} in the beam may reach the maximum interlaminar shear strength of the material even if σ_{max} is quite low. Thus, a flexural specimen of small L/d ratio in three-point bending will fail in the interlaminar shear mode by cracking along

TABLE II Mechanical property values for laminated, multi-layer composites containing 0.8 vol % of BK10 unidirectional glass fibre (15.0 ± 2.3 μm diameter). Experimental values are average of three individual specimens

Specimen ID	Deflection[a] (mm)	Young's modulus (GPa)	Work of fracture (kJ m^{-2})	Flexural strength[b] (MPa)
PMMA	3.9	2.85 ± 0.09	52.8 ± 16.2	116.0 ± 3.8
(CCPP)s	2.6	4.95 ± 0.13	16.3 ± 1.1	131.8 ± 5.0
(CPCP)s	2.9	4.07 ± 0.11	14.2 ± 1.1	110.8 ± 6.7
(CPPC)s	3.0	4.01 ± 0.14	15.0 ± 2.3	101.4 ± 0.9
(PCCP)s	3.2	3.31 ± 0.07	37.1 ± 1.0	140.8 ± 1.0
(PCPC)s	3.4	3.06 ± 0.05	37.4 ± 1.7	132.5 ± 2.0
(PPCC)s	3.5	2.82 ± 0.05	63.6 ± 19.3	121.8 ± 2.8

[a] Calculated by finite element method for 25 kg load.
[b] Calculated from Equation 1.

TABLE III Stress (MPa) at several nodes at flexural load of 25 kg

	1st layer[a]		2nd layer		3rd layer		4th layer	
	bottom	upper	bottom	upper	bottom	upper	bottom	upper
PMMA	70.8[a]							
(CCPP)s	124.9			113.7	45.9[b]			
(CPCP)s	137.6	131.5	52.9[b]					
(CPPC)s	142.0	136.0	54.7[b]					
(PCCP)s	61.9	26.7[b]	81.6			67.0	28.7	
(PCPC)s	64.4	27.8[b]	85.0	78.7	32.5			
(PPCC)s	67.4[b]							

[a] Layer sequence is numbered from the bottom tensile face to the neutral axis.
[b] Stress where initial failure is believed to have occurred.

TABLE IV Stress (MPa) at several nodes at failure load

	1st layer[a]		2nd layer		3rd layer		4th layer	
	bottom	upper	bottom	upper	bottom	upper	bottom	upper
PMMA	111.8[b]							
(CCPP)s	245.6			223.7	90.1[b]			
(CPCP)s	227.0	216.7	87.2[b]					
(CPPC)s	237.0	226.3	91.0[b]					
(PCCP)s	140.7	60.9[b]	186.0			157.9	65.2	
(PCPC)s	130.3	56.5[b]	172.6	159.5	65.8			
(PPCC)s	144.1[b]							

[a] Layer sequence is numbered from the bottom tensile face to the neutral axis.
[b] Stress where initial failure is believed to have occurred.

a horizontal plane between the laminae [9]. Therefore, the L/d ratio should be large enough to cause tensile fracture for calculating the flexural strength. In the present study, all fractures commenced in the tensile mode, thus, the L/d ratio of 12 is reasonable for the flexural strength calculations and fractographic study.

Most of the multi-layer composites failed first by tensile fracture followed by delamination (shear failure). Most specimens shown in Fig. 1(b) had an initially flat fracture surface, indicating tensile fracture, followed by delamination where the shear stress exceeded the shear strength of that layer and the crack propagated along the fibre direction causing the matrix to separate from the fibre. This delamination propagated in both directions, left and right from the midpoint. After delamination, cracks propagated perpendicular to the fibre direction in the tensile fracture mode resulting in complete fracture. The delamination is due to the large interlaminar shear stress developed within the laminae in flexure.

The delamination at the neutral axis after the initial tensile fracture depended upon what layer is at that neutral axis. For the specimen containing the composite layer(s) at the neutral axis such as (PPCC)s, (PCPC)s and (CPPC)s, as the crack approaches the neutral axis, it moves into a field of decreasing tensile stress and increasing interlaminar shear stress, the tensile fracture stops and the crack propagates in the fibre direction such that the fibres debond from the matrix. The delamination and failure cause the neutral axis to move upward toward the compressive surface (top) and failure recommences as a tensile failure. The initial fracture in PMMA starts in the tensile zone rather than the compressive zone because the compressive strength (131 MPa [10]) of PMMA is higher than the tensile strength (76 MPa [10]). When a PMMA layer was at the neutral axis (eg. (CPCP)s and (PCCP)s), delamination did not occur at the neutral axis, the crack passed upward through the neutral axis in the tensile fracture mode until reaching a composite layer.

In these multi-layered composites, delamination occurring before ultimate failure can be observed, because of the specimen's optical transparency. Once tensile fracture commenced, it led to catastrophic failure. Therefore, any delamination occurring after tensile fracture does not affect the load-deflection curve very much. As shown in Fig. 5, the deflection curves did not show any breaks or deflections typical of delamination up to ultimate failure.

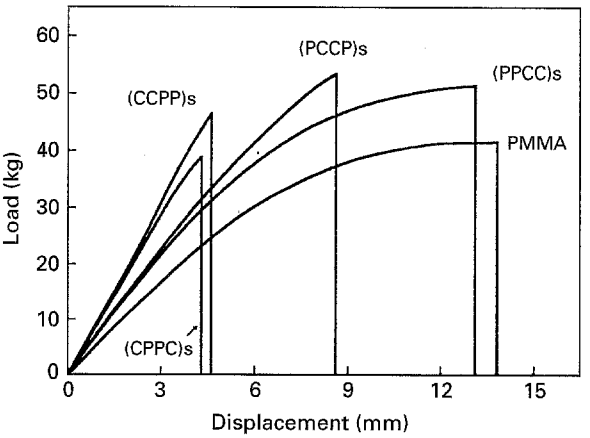

Figure 5 Load versus displacement curves for multi-layered composites and PMMA tested in three-point bending. Composites contain 0.8 vol % of unidirectional BK-10 glass fibres. Test specimen length = 10 cm, span = 8 cm and breadth = 1 cm.

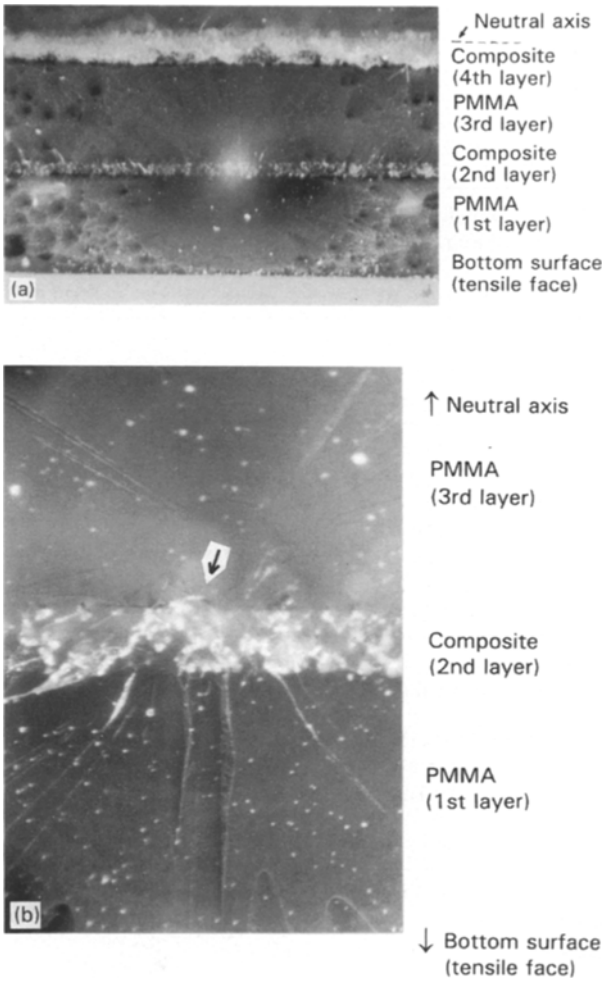

Figure 6 Fracture surface for (PCPC)s specimen showing fracture initiation point at the upper part of the 1st layer-PMMA (bright spot). Notice that fracture did not initiate at the bottom surface. Magnification of (a) is 19×. (b) is a magnified view (86×) of the region at the bright spot in (a).

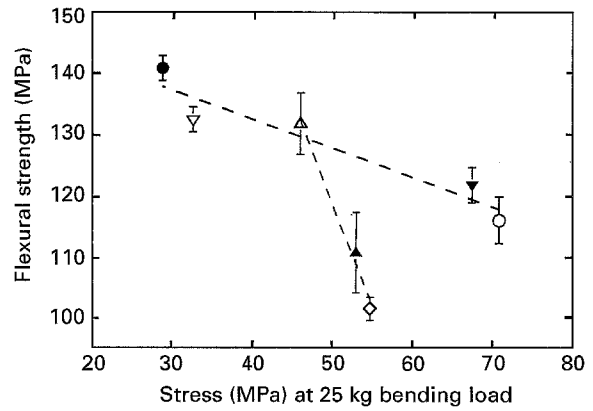

Figure 4 Flexural strength as a function of the stress, at 25 kg load, in that layer where failure is believed to have started. △ (CCPP)s; ▲ (CPCP)s; ◇ (CPPC)s; ● (PCCP)s; ▽ (PCPC)s; ▼ (PPCC)s; ○ PMMA.

From the stress distribution shown in Fig. 3, calculated by FEM, and in Table III, it is expected that the initial crack for the (PCCP)s and (PCPC)s samples did not initiate at their outermost layer because the highest stress doesn't occur at the outer layer. Fracture started at the PMMA layer adjacent to that composite layer which experienced the highest stress rather than at the composite layer or interface. For example, in the (PCPC)s sample shown in Fig. 6(a), the crack initiated close to the composite layer (2nd layer) where the tensile stress was highest, see Table IV and Fig. 3(e). The fracture then propagated vertically through the specimen in both directions, up and down. A magnified view of the crack initiation area in Fig. 6(b) makes it clear that the crack initiated at the top (indicated by arrow) of the 1st layer-PMMA. The fracture surface for the (CCPP)s sample is shown in Fig. 7. In Fig. 7 the circular mirror region shows that the fracture commenced at the bottom of 3rd layer-PMMA, right above the interfaced of the 2nd layer-composite and 3rd layer-PMMA. The fracture surface of the PMMA shows the morphology typical of a normal fracture surface. Near the fracture origin, a circular mirror-like surface is generally observed, which becomes increasingly rougher with distance from the crack origin.

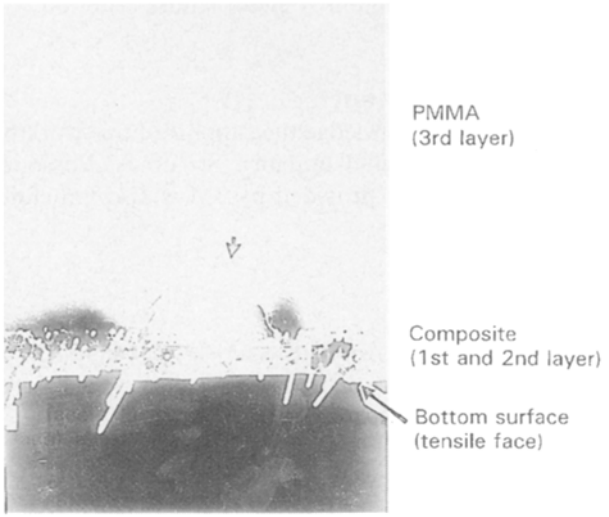

Figure 7 Fracture surface for (CCPP)s specimen showing crack initiation at the bottom of 2nd layer-PMMA. Magnification is 50 ×.

An oblique view of the fracture surface for a (PCCP)s sample is shown in Fig. 8. Note that the orientation of the sample in Fig. 8 is such that the tensile region in this sample is at the top of the photograph. Crack initiation started at the 4th layer-PMMA, passed through the neutral axis and then stopped at the composite layer in the compressive zone. In this composite layer, debonding of the fibre from the PMMA matrix occurred. This debonding of the fibres is attributed to weak interfacial bonding. It should be recalled that no coupling agent, which chemically bonds the glass fibre to the PMMA matrix, was used in these samples.

When the stress at the failed layer exceeds the strength of that layer, maximum stress failure theory can be applied. Table IV shows the stress distribution

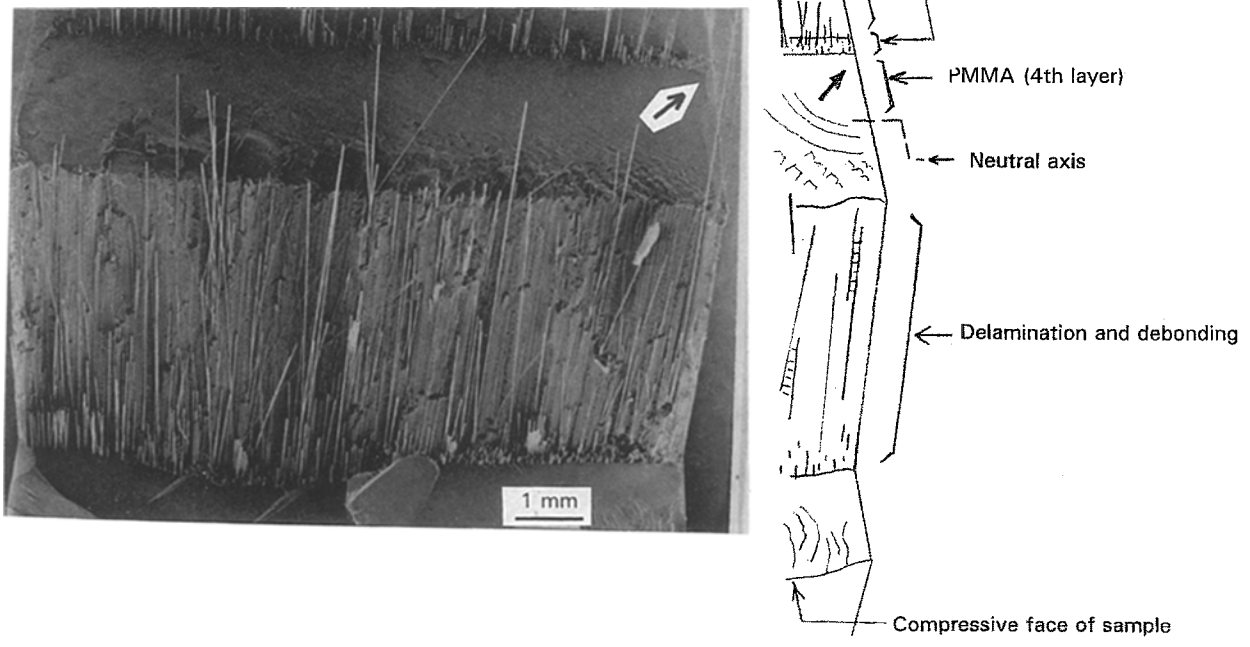

Figure 8 Oblique view of fracture surface for a (PCCP)s specimen. White bar is 1 mm.

at the breaking load and the layer (marked with a 'b') where fracture initiated. For PMMA, the average flexural strength was 116 MPa (literature value is 110 MPa [10]) which agrees reasonably well with the calculated stress at failure of 111.8 MPa in Table IV. However, in the multi-layer composites, the stresses in the PMMA layer at initial fracture ranged from 60.9 MPa for (PCCP)s to 144.1 MPa for (PPCC)s in Table IV. This relatively large scatter suggests that the simple maximum stress criterion cannot be applied even though the initial fracture mode was a tensile fracture.

4. Conclusions

Laminating prepregs, which contain glass fibres and PMMA of matched refractive index and where the fibres were coated with the PMMA polymer, to thick PMMA plates produced composites with an optical transmission of 80 to 90% between 22 and 46 °C in the visible range, 450 to 700 nm. Changing the stacking sequence of the PMMA plates and composite layers was important to the flexural properties, but the optical transmission remained the same. With only 0.8 vol % fibre, the (CCPP)s sandwich structure had the highest Young's modulus as expected, but the (PCCP)s structure had a higher flexural strength. The flexural strength increased by 21% (for the (PCCP)s specimen) while the modulus of elasticity increased by 74% (for the (CCPP)s specimen) compared to PMMA. This is an impressive improvement considering the low fibre content of only 0.8 vol % and that no coupling agent was applied to these fibres. These differences are not due to inherent properties of the materials, but to the stacking sequence which makes optimum use of the elastic properties of each material.

Stress distributions under flexural loading were calculated using the FEM and it allowed the position of initial failure to be established. Fracture initiated near the point of highest stress, so the fracture did not always start at the outer surface of the sample. The flexural strength is related to the stress level created during flexure. In each group, P-out and C-out, a specimen experiencing a higher stress had a higher probability of fracture. Thus, its flexural strength was lower than that of other specimens containing lower stresses under same load.

The fracture was always complex (tensile and shear), starting with tensile failure followed by shear mode (delamination) and another tensile mode. The first crack always commenced at a PMMA layer adjoining the composite layer which contained the highest stress. The computed stresses for the PMMA layers at failure ranged from 56.5 to 144.1 MPa. This relatively large deviation (scatter) from the reported flexural strength (116 MPa) of PMMA made it impossible to apply simple maximum strength failure criterion.

Acknowledgement

The authors acknowledge the support of this work by McDonnell Aircraft Company, St. Louis, Missouri. The PMMA sheet provided by 3M is also gratefully acknowledged.

References

1. H. LIN, D. E. DAY and J. O. STOFFER, *Polymer Eng. Sci.* **32** (1992) 241.
2. S. KANG, H. LIN, D. E. DAY and J. O. STOFFER, *J. Mater. Res.* (1996) in press.
3. R. K. SIX, J. O. STOFFER and D. E. DAY, *Polym. Mater. Sci. Eng. Prepr.* **65** (1992) 223.
4. A. F. JOHNSON and G. D. SIMS, *Composites* **17** (1986) 321.
5. E. J. VAN VOORHEES and D. J. GREEN, *J. Amer. Ceram. Soc.* **74** (1991) 2747.
6. H. G. TATTERSALL and G. TAPPIN, *J. Mater. Sci.* **1** (1966) 296.
7. W. WATT and B. V. PEROV, in "Strong fibres", Vol. 1 (Elsevier Science Publishers, Amsterdam, North-Holland, 1985) p. 45.
8. G. L. HANNA and S. STEINGISTER, in "Composite materials, testing and design" (STP 460 ASTM, Philadelphia, PA 1976) p. 182.
9. J. V. MULLIN and A. C. KNOELL, *Materials Research and Standard* **December** (1970) 16.
10. Plexiglas® Design, & Fabrication Data, PL-1p, Philadelphia, PA, Rohm and Haas Company (1983) 6.

Received 10 August
and accepted 21 December 1995